LCF BEHAVIOR AND LIFE EVALUATION OF A SINGLE CRYSTAL NICKEL BASE SUPERALLOY UNDER DIFFERENT DWELL CONDITIONS

Hui Chen YU*, Ying LI, Shi Chao ZHANG, Xue Ren WU
Beijing Key Laboratory of Aeronautical Materials Testing and Evaluation, National Key Laboratory of Science and Technology on Advanced High Temperature Structural Materials, Beijing Institute of Aeronautical Materials, Beijing 100095, China.
**yhcyu@126.com;*

Keywords: *Crystallographic orientation; Low cycle fatigue; Life prediction; Single crystal superalloy; Strain dwell.*

Abstract

Low cycle fatigue (LCF) tests were conducted at elevated temperatures of 760ºC and 980ºC under different dwell conditions on a single crystal nickel base superalloy. The specimens, which have crystallographic orientations near [001], [011] and [111], were tested under total fully reversed axial strain control. The experimental results indicated that the fatigue life-strain amplitude curves were temperature, crystallographic orientation and strain dwell dependent. When strain range was lower than 2% for [001] orientation, the fatigue life was longer at 760ºC and shorter at 980ºC for the same strain rang. However, when strain range was higher than 2% for [001] orientation, the reverse result was obtained. The longest fatigue life was observed for specimen with [001] orientation, while the shortest one for specimen with [111] orientation mainly due to variations in Young's modulus with orientations. Compared with continuous cycling tests without strain dwell, the ones with tensile, compressive or tensile-compressive strain dwells showed some shorter fatigue lives. The difference of fatigue lives under different strain dwells reflects the fatigue-creep interactions at elevated temperature. The cyclic deformation and life distribution features were analysed and modified Cyclic damage accumulation (CDA) method was proposed to evaluate the fatigue life of the alloy. The prediction agrees well with the experimental results.

1 Introduction

The efficiency of gas turbine for jet engine relies in part on the temperature capability of turbine blade and vane material. The design of advanced jet engine with improved performance has led to the development of single crystal nickel base superalloy blade. Such alloy is superior to conventionally cast superalloy, because the elimination of the grain boundaries enhances elevated temperature ductility and single crystal casting process provides a preferred low modulus [001] texture orientation parallel to the solidification direction. The minor alloying elements used as grain boundary strengtheners are no longer useful here and act to reduce the incipient melting temperature. These result in a high creep strength and ductility as well as fatigue resistance [1, 2].

Turbine blade material is subjected during service to complex thermal and mechanical loads. The blade root where the blade is attached to the turbine disc is primarily a cyclically loaded notched member. The combination of these factors can lead to high temperature LCF with possible fatigue-creep interaction [3-5]. High temperature LCF and creep-fatigue interaction resistances are considered to be the mechanical properties of major concern. The development of a life prediction procedure requires a proper understanding of LCF damage mechanisms

under isothermal conditions in the temperature range of actual component cycles [4, 5].

The present study is devoted to the LCF and fatigue-creep interaction behaviors of a single crystal nickel base superalloy. The influences of temperature, crystallographic orientation and loading type with and without straindwell on LCF life have been investigated.

2 Material And Experimental Procedures

2.1 Material and Specimen

The material studied is a single crystal nickel base superalloy with high γ′ volume fraction. The chemical compositions (wt%) of the material are 0.01C, 4.4Cr, 9.0Co, 8.0W, 1.8Mo, 5.8Al, 0.6Nb, 7.2Ta, 2.2Re, 0.1Hf and balance Ni. The alloy was directionally solidified along the natural dendrite direction [001] in the form of single crystal cylinder 15 mm in diameter and 100 mm in length. The same size cylinder was also cast with an axial direction near [011] or [111] corners. The crystallographic orientation of the round bar was measured by Laue back reflection X-ray technique. The maximum deviation of the rod axis from [001], [011] or [111] direction was layed within 10º. All of the bars were fully heat treated, i.e. solution heat treatment (1290°C/1h + 1300°C/2h + 1315°C/4h/AC), and two stages of ageing heat treatment (1120°C/4h/AC + 870°C/32h/AC).

Fig. 1 shows a SEM image of the cross section of the bar with [001] orientation after heat treatment. The alloy microstructure consists of regularly packed cuboidal γ′ particles in a face-centred cubic (fcc) γ matrix. The γ'/γ arrangement in the whole volume is quite regular with the mean size of the γ′ particles about 400 nm. The volume fraction of γ′ particles is approximately 65%. The gray areas in Fig. 1 disturbing the regular cuboidal appearance represent horizontal sections right through particular γ matrix channels.

Button-ended cylindrical specimens with a gauge diameter 6 mm, gauge length 14 mm and total length 90 mm were machined from heat-treated bars. The crystallographic orientation of [001], [011] and [111] was aligned parallel to the specimen axis. The mechanical properties in [001] orientation of the alloy after heat treatment at different temperatures are shown in Table 1, which were obtained by using standard tensile specimen. The Yong's modulus of the alloy decreases with temperature increasing. However, the yield stress is nearly unchanged during temperature changing from room temperature to 760˚C. When temperature increases to 850˚C, the yield stress reaches its maximum value 1030MPa. But the yield stress decreases obviously after temperature is over 850˚C.

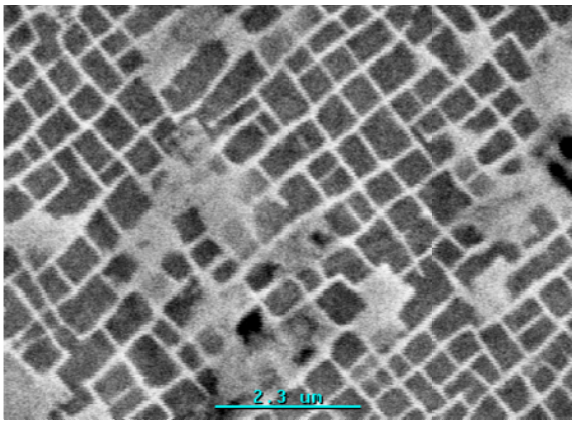

Fig. 1. Microstructure of the alloy after heat treatment.

Table 1. Mechanical properties of the alloy.

Temperature [℃]	σ_b [MPa]	$\sigma_{0.2}$ [MPa]	E [GPa]
25	970	930	132
650	1060	940	108
700	1030	930	107
760	1100	935	106
850	1070	1030	98
980	800	680	81
1070	545	440	70
1100	540	385	68

2.2 Experimental Procedures

The tests were performed on a a closed-loop servohydraulic test machine (Shimazu EHF-100KN-20L) under total strain control in symmetrical push-pull at a constant strain rate of $5x10^{-3}s^{-1}$. The tests were carried out at temperatures of 760˚C and 980˚C. Specimens were heated with a radiation furnace to give

temperature gradients within ±2˚C over the specimen gauge length.

A triangular waveform command signal, with the option of introducing strain dwell periods at tensile peaks or compressive valleys, was used during the tests. There were four different types of loading, namely continuous cycling (denoted as 0/0), cycling with a tensile strain dwell (t/0, t=60s), a compressive strain dwell (0/t, t=60s) and balanced strain dwells (t/t, t=30s). Throughout the tests, a continuous record was made of the load-time and strain-time history to monitor the cyclic hardening/softening response. Hysteresis loops were also recorded regularly throughout the tests by computer. The load wave with tensile strain dwell is shown in Fig. 2. Strain was measured with a high temperature axial extensometer in 12mm gauge length. Specimen failure was defined as specimen rupture or as a reduction of the stabilized maximum cyclic stress range by 30%. TEM observations were conducted through JEOL 2000FX facility. TEM foils were made from the samples which were cut within gauge section either perpendicular or parallel to the axis of the specimens.

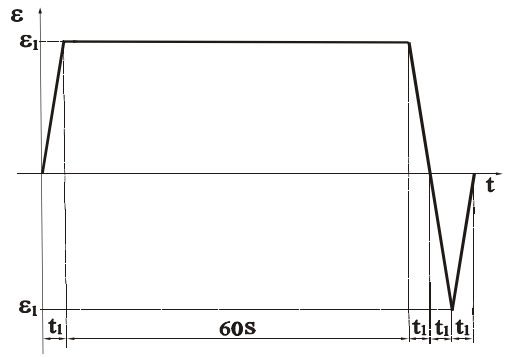

Fig. 2. Load waves with tensile strain dwell.

3 Results and Discussions

3.1 Cyclic Stress-Strain Behavior

The cyclic stress-strain response is an important aspect in LCF studies since it reflects the true stress-strain characteristic of a material under LCF condition. Fig. 3 shows the cyclic stress-strain response of the single crystal alloy with [001], [011] and [111] orientations under 760°C and 980°C. The cyclic stress-strain data were derived through hysteresis loops of 50 pct of cyclic life (N_f /2) and they can be expressed approximately by Eqn. 1.

$$\frac{\Delta\varepsilon}{2}=\frac{\Delta\sigma}{2E}+\left(\frac{\Delta\sigma}{2K'}\right)^{1/n'} \qquad (1)$$

Where $\Delta\varepsilon$ is total strain range, $\Delta\sigma$ is total stress range, E is Young's Modulus, K' and n' are cyclic strength coefficient and cyclic strain hardening index. In Fig. 3, the symbols represent experimental data of cyclic stress-strain response and the lines are calculated values by Eqn. 1. The experimental data are correspondence well with calculated values. Parameters K' and n' are determined by regression analysis to the stress-strain data and are shown in Table 1 for different temperatures and orientations, respectively.

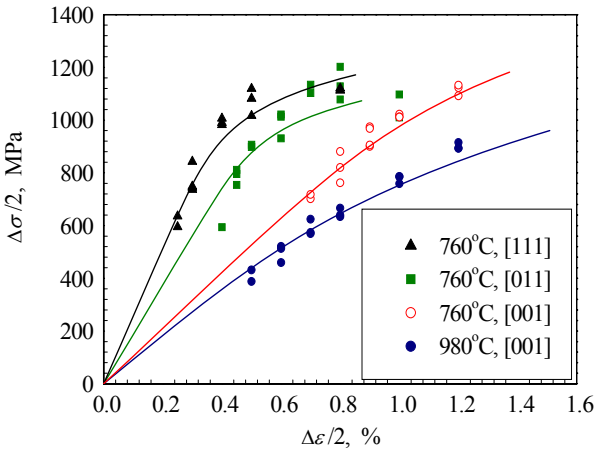

Fig. 3 Cyclic stress-strain curves at different temperatures

Table 1 LCF parameters at different temperatures

Temperature ,°C	Orientation	K'	n'
760	[001]	3022	0.157
980	[001]	3813	0.257
760	[011]	1816	0.091
760	[111]	2086	0.104

The test results reveal temperature and orientation affections on cyclic stress-strain behavior. At 760°C, the stress amplitude is the highest with [111] orientation and the lowest with [001] one for the same strain amplitude.

The stress amplitude at 760°C is higher than that at 980°C with the same orientation [001].

3.2 LCF Stress-Life Response

During LCF experiments, the changes of stress values with cyclic numbers were recorded at a given strain amplitude. Fig. 4 and Fig. 5 show the cyclic total stress range as a function of cyclic numbers measured in experiments with different strain range. Fig. 4 is the case of the alloy with [001] orientation tested at 760˚C, the alloy represents cyclic hardening within the first ten cycles and the degree of hardening decreases with strain range decreases. The cyclic stress response is nearly constant at 760˚C when strain range is of 1.4%. When strain range is higher than 1.4%, a saturation stage occurs after the initial hardening until the final failure. Fig. 5 is the case of the alloy with [001] orientation tested at 980˚C, the alloy represents cyclic softening and the degree of softening decreases with strain range decreases. It is similar to the case at 760˚C, the cyclic stress response is nearly constant at 980˚C when strain range is of 1.0%. When strain range is higher than 1.0%, a saturation stage occurs after the initial softening until the final failure. The cyclic stress response decreases quickly before the final fracture of the alloy at both temperatures. It means the macro crack forming and propagating to failure soon.

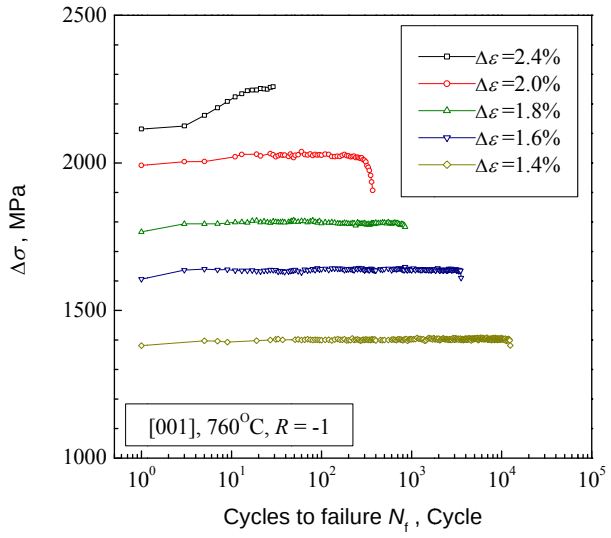

Fig. 4 Cyclic stress response with [001] orientation at 760˚C

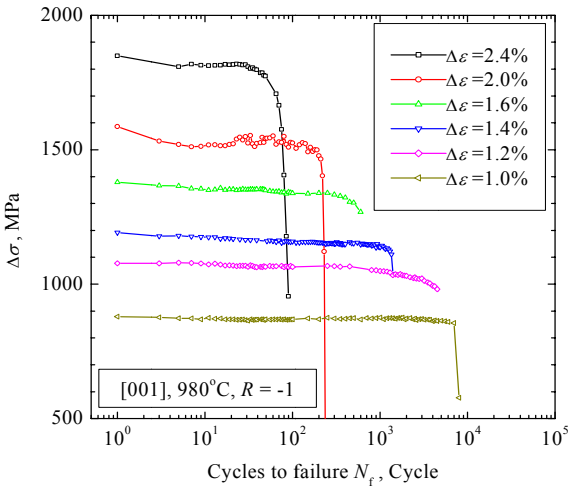

Fig. 5 Cyclic stress response with [001] orientation at 980˚C

When LCF test performed at 760˚C, the shape of γ′ phase hardly changed. Dislocations formed and piled up or crowded in the γ matrix phase first. γ′ particles were frequently cut by dislocation pairs. The increasing of dislocations resulted in interactions among dislocations, as well as between dislocations and γ′ particles, shown as in Fig. 6. The sample in Fig. 6 was tested at the conditions of R=-1 and $\Delta\varepsilon$=2.4%. Further moving of dislocations was blocked and leaded to cyclic hardening, as shown in Fig. 4.

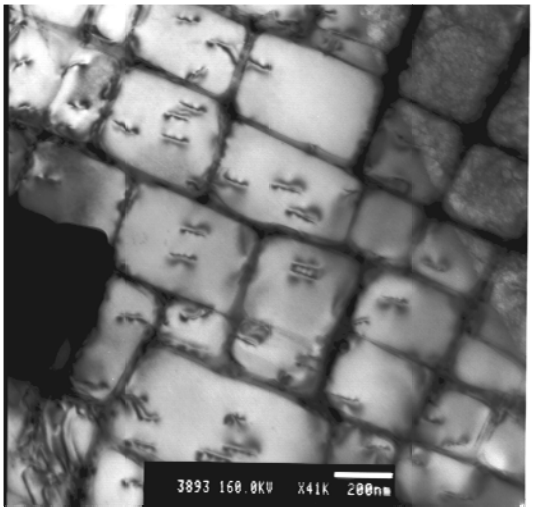

Fig. 10 Microstructure of the alloy tested at 760 °C, $\Delta\varepsilon$=2.4%, [001]

However, when LCF test performed at 980˚C, the non-planar arrangement of dislocations in sample, implying that thermally activated cross slip had taken place at high

temperature, and some dislocations climbed over γ′ phases and the alloy represented cyclic softening behavior at 980˚C, shown as in Fig. 7. The test results also show that the alloy generally represents cyclic hardening and the hardening degree decreases with strain range decreases, no matter which orientation the alloy is with when tested at 760˚C. At both temperatures, a saturation stage occurs until the final failure after initial cyclic hardening or cyclic softening. This is because that a homeostasis between dislocation formation and dislocation annihilation was attained, as shown in Fig. 4 and Fig. 5.

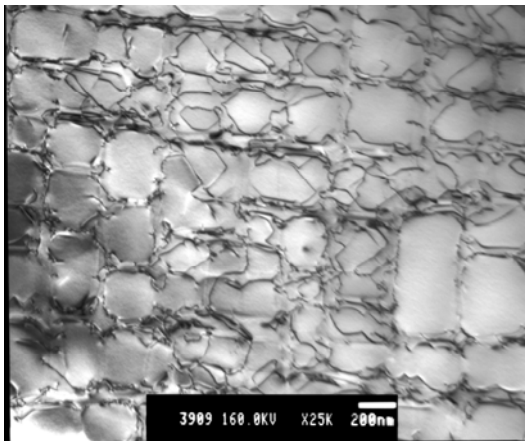

Fig. 7 Microstructure of the alloy tested at 980 °C, $\Delta\varepsilon$=2.4%, [001]

3.3 LCF Life Behavior

3.3.1 Temperature effect on LCF Life

The influence of temperature on LCF life of the single crystal alloy with [001] orientation is illustrated in Fig. 8. The cyclic total strain range at 760°C and 980°C as a function of cyclic numbers to failure measured in experiments is shown in Fig. 8. The □ and ○ symbols express the test data at 760°C and 980°C, respectively. The relationship between cyclic total strain range $\Delta\varepsilon$ (%) and cyclic numbers o to failure N_f (cycle) is approximated by Coffin-Mansion power equation [6], which is also shown in Fig. 8 with dash line for 760°C and solid line for 980°C.

The results indicate that, unlike the temperature dependence of yield stress which sharply decreases in the temperature range varying from 760°C to 980°C, fatigue life of the alloy at 980°C is comparable to or slightly higher than those at 760°C when strain range higher than 2%. Generally, at different strain range, the temperature dependence of fatigue life has different trend. At lower strain range (lower than 2%), LCF life at 980°C is shorter than that at 760°C, and the contrary is the case at higher strain range (higher than 2%). In other words, LCF life is more sensitive to the strain range at 760°C. This may be the result of different cumulative damage mechanism at different temperatures of the alloy. It can be seen from the hysteresis loop that more plastic deformation was borne on specimen at 980°C under the same strain amplitude, which means that an increment on the strain range results in a smaller increment on the stress range at 980°C.

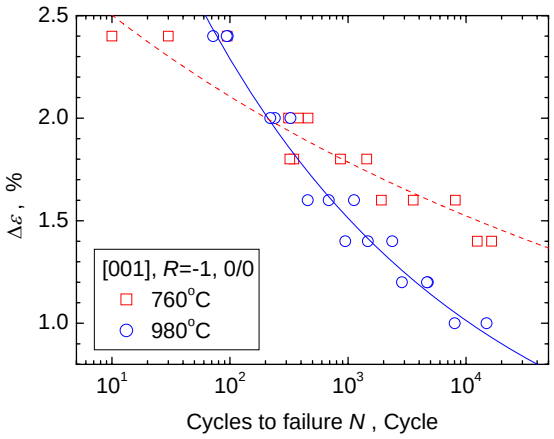

Fig. 8 LCF life at different temperatures.

3.3.2 Orientation effect on LCF Life

LCF life at 760°C as a function of strain range and orientation is displayed in figure 4. LCF life was highly orientation dependent at this intermediate temperature. Fatigue lives with [001] and [111] orientation represent the upper and lower bounds, respectively. The similar results were reported by Chieratti [3] and Li [4, 5] in that LCF life of single crystal, Mar-M200 and SRR99. This behavior is mainly due to variations in Young's modulus with orientation. At 760°C, The Young's moduli are 105.5GPa, 187.5GPa and 223.3GPa for [001], [011] and [111] orientations. The Young's moduli are very

different with varied orientations. A satisfactory correlation was obtained when fatigue life was taken as a function of stress range at 50 pct of cyclic life (N_f /2), shown as in Fig. 10. The orientation affection can be decrease and no significant consistent orientation dependence. t

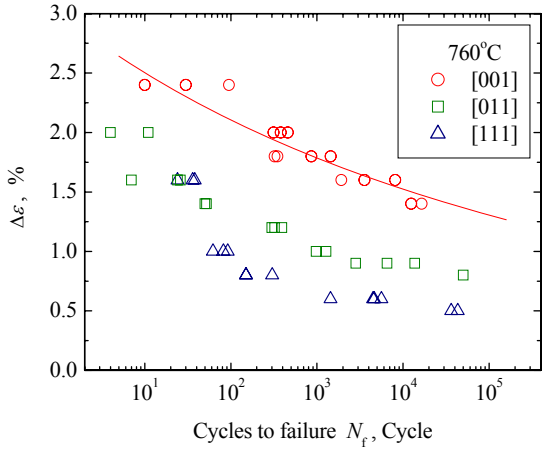

Fig. 9 Fatigue life on a strain amplitude basis at 760°C

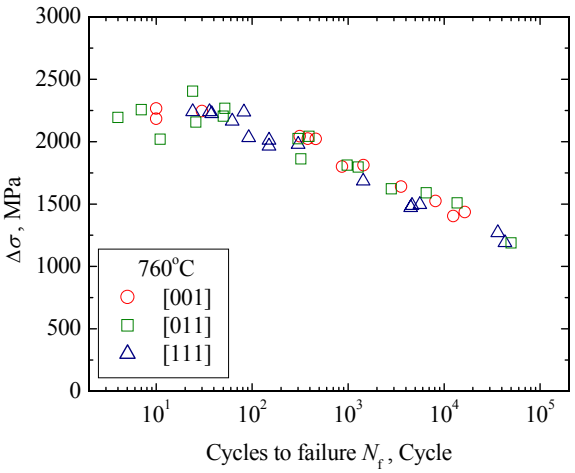

Fig.10 Fatigue life on a stress amplitude basis at 760°C

3.3.3 Strain dwell effect on LCF Life

It has been found that strain dwell have an obvious effect on the LCF life for different materials [4, 5]. Both tensile and compressive strain dwell result in more damage of material as fatigue-creep interaction. However, various materials and different temperatures may results in conflicting arguments. The study on single crystal SRR99 indicates that the influence of hold (dwell) time on fatigue life is strongly dependent on temperature [4, 5], which was attributed to their effect on crack initiation and crack propagation.

The specimens of the present alloy studied with [001] orientation always exhibites shorter fatigue life with strain dwell compared with specimens without strain dwell at different temperatures of 760°C and 980°C, regardless of the type of loading, as shown in Fig. 11 and Fig.12,. This means that both of tensile dwell and compressive dwell has additional damage to the alloy. On the other hand, such an influence on fatigue life may be related to the change of frequency. As well known, high frequency corresponds to low fatigue life. In this study the total dwell time is 60s, one cycle period with strain dwell increases by more than one order of magnitude. In addition, strain dwell may affects the cyclic deformation in the following aspects: mean stress with tensile dwells generating compressive mean stress and with compressive dwells generating tensile mean stress, inelastic strain, time dependent creep damage and oxidation. All of these factors enhance fatigue crack initiation and propagation. By comparing different strain dwell types from Fig. 11 and Fig.12, it can be observed that the combined results for tensile strain dwell, compressive strain dwell and tensile-compressive strain dwell are substantially the same.

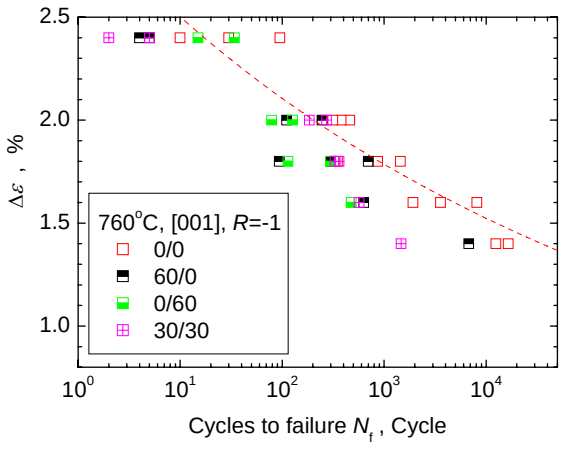

Fig. 11. Strain range-life curves with different strain dwell at 760°C.

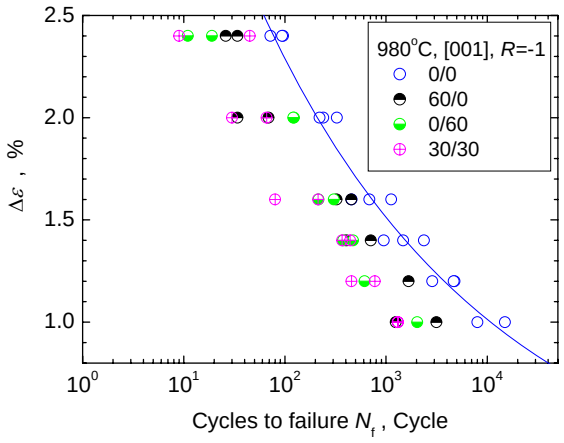

Fig. 12 Strain range-life curves with different strain dwell at 980°C.

3.4 LCF Life Prediction

Cyclic damage accumulation (CDA) method was used by NASA for fatigue-creep life prediction [7, 8]. In the present study, a modified CDA method was used to predict the life of the single crystal superalloy, which can be expressed by Eq. 2.

$$N_f = 10^{\left[A+n_1 \log_{10}^{\Delta\sigma}+n_2\sigma_m\right]} \times 10^{\left[n_3\Delta\varepsilon/f(A_{hkl})+n_4\sigma_{\max}+n_5 t_t+n_6 t_c\right]} \quad (2)$$

where A, n_1, n_2, n_3, n_4, n_5 and n_6 are material constants. $\Delta\varepsilon$ is total strain range, $\Delta\sigma$ is total stress range, σ_m is mean stress, σ_{max} is the maximum stress. t_t is tensile strain dwell time, t_c is compressive strain dwell time. $f(A_{hkl})$ is orientation function, its value is 1 for the case of [001] orientation, 0.25 for [011] orientation and 0.33 for [111] orientation. $f(A_{hkl})$ can be expressed by Eq. 3.

$$f(A_{[hkl]}) = 1 - \left(2 + 2\nu_{[001]} - \frac{E_{[001]}}{G_{[001]}}\right) A_{[hkl]} \quad (3)$$

$A_{[hkl]}$ is orientation parameter, , which can be expressed by Eq. 4.

$$A_{[hkl]} = \frac{h^2k^2 + k^2l^2 + l^2h^2}{\left(h^2 + k^2 + l^2\right)^2} \quad (4)$$

h, k, l are values of orientation index.

The prediction values and test data are shown in Fig. 13 of 760°C and in Fig. 14 of 980°C. It reveals a good correlation between calculated value and test data (±2 times), no matter the specimen axis is parallel to any crystallographic orientation of [001], [011] and [111]. This fact suggests that the fatigue life of the present alloy can be predicted reasonably well by using modified CDA method.

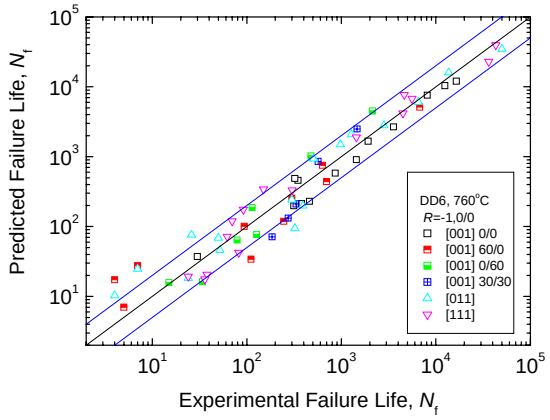

Fig. 13 Prediction results by CDA method vs. test data at 760°C

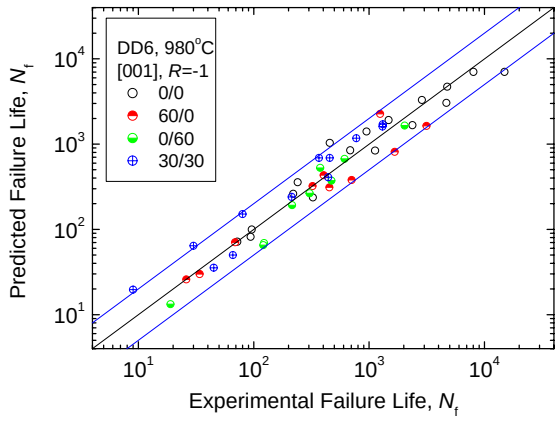

Fig. 14 Prediction results by CDA method vs. test data at 980°C

4 Summary

(1) The fatigue life-strain curves of the alloy were temperature dependent. When strain

range was lower than 2% for [001] orientation, the fatigue life was longer at 760ºC and shorter at 980ºC for the same strain range. However, when strain range was higher than 2%, the reverse result was obtained.

(2) At 760 ºC, the alloy generally represents cyclic hardening within the first ten cycles and the degree of hardening declines with strain range decreases. At 980 ºC, the alloy generally represents cyclic softening and the degree of softening declines with strain amplitude decreases. Most of dislocations were formed firstly in γ matrix and then expanded into γ′ phase at 760ºC or climbed over γ′ phase at 980ºC.

(3) The crystal orientation has a great influence on fatigue life. The longest fatigue life was observed for specimen with [001] orientation, while the shortest one for specimen with [111] orientation. It mainly due to variations in Young's modulus with orientations.

(4) Compared with continuous cycling test, the one with tensile, compressive or tensile-compressive strain dwell showed some shorter life. Modified CDA method gives a good evaluation of LCF life.

References

[1] Sims, C. T., Stoloff, N. S. and Hagel, W. C. *Superalloys*. A Wiley-Interscience Publication, New York. 1987.

[2] Davis JR editor. *Heat-Resistant Materials, ASM Specialty Handbook*. The Materials Information Society, 1997.

[3] Chieragatti R, Remy L. Influence of orientation on the low cycle fatigue of Mar-M200 single crystals at 650 ºC: I-Fatigue life behavior. *Mater. Sci. Eng*. 1991; A141: 1-9.

[4] Li SX, Smith DJ. High temperature fatigue-creep behaviour of single crystal SRR99 nickel base superalloys: Part I - Cyclic mechanical response. *Fatigue Fract. Engng Mater. Struct*. 1995; 18: 617-629.

[5] Li SX, Smith DJ. High temperature fatigue-creep behaviour of single crystal SRR99 nickel base superalloys: Part II – Fatigue-creep life behaviour. *Fatigue Fract. Engng Mater. Struct.* 1995; 18: 631-643.

[6] Suresh S. *Fatigue of Materials*. Cambridge: Cambridge University Press, 1991.

[7] Nelson RS, Levan GW, Harvey PR. Creep fatigue life prediction for engine hot section materials (isotropic). *NASA-CR-189221, N93-18578*, 1993.

[8] Nissley DM, Meyer TG. Life prediction and constitutive models for engine hot section anisotropic materials program. *NASA-CR-189222, N92-31534*, 1992.

Copyright Statement